begell house, inc.

Journal Production
50 Cross Highway
Redding, CT 06896
Phone: 1-203-938-1300
Fax: 1-203-938-1304
Begell House Production Contact : journals@begellhouse.com

Article Reference #: JPM1303-1374
Date Proof Sent: February 12, 2010
Total Pages: 13

Journal: Journal of Porous Media

Year: 2010 **Volume**: 13 **Issue**: 03

Article Title: On the Prediction of an Average Droplet Size Evolution During Transport in Homogeneous Porous Media Under Laminar Flow Conditions

Dear Dr. Frank A. Coutelieris:

Please review the attached PDF file which contains the author proof of your article. If you are unable to access this file, please let me know and I will fax your proof.

This is your only opportunity to review the editing, typesetting, figure placement, and correctness of text, tables, and figures. Answer copyeditor's queries in the margin. Failure to answer queries will result in the delay of publication of your article, so please make sure they are all adequately addressed. **You will not be charged for any corrections to editorial or typesetting errors; however, you will be billed at the rate of $25 per hour of production time for rewriting, rewording, or otherwise revising the article from the version accepted for publication ("author's alterations"); any such charges will be invoiced and must be paid before the article is published.**

Please return your corrections in one of the following ways: (1) Fax: Clearly mark your corrections on the page proofs and fax the **corrected pages only**, along with the offprint order form, if applicable. (2) E-mail: Indicate your corrections in a list, specifying the location of the respective revisions as precisely as possible.

Please read the instructions carefully and **if possible** email your corrections to me within 48 hours (not including weekends). If you need more time, please let me know at your earliest convenience. No article will be published without confirmation of the author's review. If we do not hear from you within the allotted time, we will be happy to hold your article for a future issue, to give you more time to make your corrections.
Attached is a form for ordering offprints, issues, or a subscription. As corresponding author, you will receive a complimentary copy of this issue. If you wish to order extra issues or offprints, please fill in the appropriate areas and fax the form to me with your corrections.

Thank you for your assistance, and please reference **JPM1303-1374** in your correspondence. Also, kindly confirm receipt of your proofs.

Sincerely,

Michelle Amoroso
Michelle Amoroso
Contact for Author Proofs

begell house, inc.

JOURNAL PRODUCTION DEPARTMENT
50 Cross Highway
Redding, Connecticut 06896
203-938-1300 (Phone)
203-938-1304 (Fax)
journals@begellhouse.com

Date: February 12, 2010

Journal Name: Journal of Porous Media

Volume/Issue #: Volume 13/Issue 03 Article #1374

Article Title: On the Prediction of an Average Droplet Size Evolution During Transport in Homogeneous Porous Media Under Laminar Flow Conditions

BILL TO:

SHIP TO:

Dear Dr. Frank A. Coutelieris:

As corresponding author, you will receive a complimentary copy of this issue. Please use the order form below to order additional material and/or indicate your willingness to pay for color printing of figures (if applicable).

To purchase individual subscriptions or a personal copy of your article, please go to www.begellhouse.com Allow approximately 3 weeks, from receipt of your page proofs, for the issue to be posted to our website. For institutional pricing on PDF files contact Meghan Rohrmann at 1-203-938-1300 or meghan@begellhouse.com

If placing an order, this form and your method of payment must be returned with your corrected page proofs. Please include cost of shipment as indicated below; checks should be made payable to Begell House, Inc., and mailed to the above address. If a purchase order is required, it may arrive separately to avoid delaying the return of the corrected proofs.

OFFPRINTS OF ARTICLE*

	PAGE COUNT OF ARTICLE (round off to highest multiple of 8)				
QTY.	4	8	16	24	32
25	72	115	151	187	223
50	84	127	163	199	236
100	108	193	254	314	375
200	156	327	435	544	652
300	205	459	616	773	930

*If your page count or quantity amount is not listed please email a request for prices to journals@begellhouse.com

Black and White Offprints: Prices are quoted above

Offprint Color Pages: Add $3 per color page times the quantity of offprints ordered

Shipping: Add 20% to black and white charge

Offprint Qty: _____ $ _____

Color Pages for Offprints: $ _____

Shipping Charges: $ _____

WIRE TRANSFER

Bank: Valley National Bank
Routing #: 0 2600 6 790
Account #: 07 011343
Swit Code: MBNY US 33

CREDIT CARD PAYMENT

CREDIT CARD # _____

NAME ON CREDIT CARD _____

AMEX/ VISA/MC/ DISC/ EURO/ _____ EXP. _____

OTHER: _____

CORPORATE PURCHASE ORDER

P. O. # _____

PAYMENT BY CHECK

INCLUDE THE FOLLOWING INFO ON YOUR CHECK:
Article Reference # and Offprints/Color/Subscription

Make checks payable to Begell House, Inc.

COST FOR COLOR PAGES PRINTED IN JOURNAL

Price Per Color Pg.: $ _____

Number of Color Pages: _____

Total Cost for Color Pages in Journal: $_____

COPY OF JOURNAL ISSUE (AUTHOR DISCOUNT)

Price Per Copy: **$**____ **Number of Copies**:_____

Total Cost for Copies: $: _____

SUBSCRIPTION — 2009

Institutional Subscription$_____*** 12 Issues Per Year** *Add $10.00 for shipments outside the United States

REVISED 3-8-09

Journal of Porous Media 13(3), xxx–xxx (2010)

ON THE PREDICTION OF AN AVERAGE DROPLET SIZE EVOLUTION DURING TRANSPORT IN HOMOGENEOUS POROUS MEDIA UNDER LAMINAR FLOW CONDITIONS

Frank A. Coutelieris*

Department of Environmental and Natural Resources Management, University of Ioannina, Seferi 2, 30100 Agrinio, Greece; and National Center for Scientific Research "Demokritos", 15310 Aghia Paraskevi Attikis, Greece

*Address all corespondence to F. A. Coutelieris E-mail: fkoutel@cc.uoi.gr

Original Manuscript Submitted: 9/11/2008; Final Draft Received: 11/28/2008

This paper deals with the prediction of a spatially averaged droplet size during transport within homogeneous porous media. More precisely, this transport process occurs in a mixture of a continuous aqueous phase which includes a discontinuous one in the form of droplets. The mixture flows in a homogeneous porous medium under laminar flow conditions. The collection of γ-order moments, $S\gamma$, is used here to describe the time evolution of the spatially averaged mean diameter of spherical droplets, mainly because $S\gamma$ satisfies the convective/diffusive transient transport equation. As it is well known, breakup and coalescence are the primary local phenomena controlling the size of droplets in such a process. The essence of the so-called "$S\gamma$ concept" is that break-up and coalescence processes determine the source terms in a transport equation for the moments of an averaged characteristic size, representative for the droplet size. The velocity vector at any point is calculated by typical computational fluid dynamics simulations. The assumptions made are that (a) the flow conditions correspond to low Reynolds numbers, (b) the local flow field is independent of the droplets and thus, the droplet size is small enough compared with the mean pore diameter, and (c) the liquid/solid interfaces are chemically neutral. Since the proposed constitutive model adequately simulates the droplet transport process, it is used here for the investigation of the effect of porous geometry and flow characteristics on the droplet size.

KEY WORDS: *multiphase transport, $S\gamma$ moment, break-up, coalescence, porous media*

1. INTRODUCTION

Transport of mixtures is encountered in many industrial processes as well as in engineering applications. More specifically, one of the most interesting cases is that of a discontinuous phase (droplets) sited in a flowing continuous aqueous one. A typical example might be a problem of interest to the oil industry, which is related to an unconventional behavior found in some heavy oil reservoirs where a disconnected gas phase (gas bubbles) inside a connected liquid phase (heavy oil) is observed over periods of time large enough to consider that such a phase distribution is governing the flow dynamics (Gerami and Pooladi-Darvish, 2007; Heibel et al., 2001). Qualitatively speaking, the aspects of such a transport process are rather well understood: in general, droplets are transferred due to convection and diffusion, while their population is strictly governed by local hydrodynamic phenomena (Sheng et al., 1999). It is very difficult to obtain a globally valid description for the consequent tran-

1091-028X/10/$35.00

NOMENCLATURE

Latin symbols

c	$= \beta^{1/2}$, artificial speed of sound
Ca_{cr}	critical capillary number
d	diameter (size) of the droplets
d'	arbitrary diameter to define a collision event
d_{32}	mean droplet diameter
d_{cr}	critical droplet diameter
d_{eq}	equivalent mean diameter of a uniform distribution
$d_{\gamma_1\gamma_2}$	characteristic diameter given by Eq. (3)
E	extinction term in Eq. (5)
$f_1(\lambda)$, $f_2(\lambda)$	interpolation functions given in Table 1
G	generation term in Eq. (5)
$h_i^{(\gamma)}$	source terms for transport Eqs. (7) and (9)
$h_{br}^{(\gamma)}$	Break-up source term
$h_{cl}^{(\gamma)}$	coalescence source term
K_{br}	Break-up rate
$K_{cl}\,(d, d')$	collision rate
$K_{cl}\,(d_{eq})$	coalescence rate
$K_{coll}\,(d_{eq})$	$= k_{coll}\,u_{rel}\,(d_{eq})$, Smoluchowski collision rate
M	Mach number
n	total number density
$N_f(d)$	number of fragments of diameter d
p	pressure field
$P(d)$	size distribution of the droplets
P_0	pressure at outlet
$P_{coal}(d_{eq})$	coalescence probability of a single collision event
$P_{\rm in}$	pressure at inlet
R	Reynolds number
r	position vector
S_γ	moments of distribution
$(S_\gamma)_{\rm in}$	moments of distribution at inlet
$(S_\gamma)_{\rm out}$	moments of distribution at outlet
t	time
$t_{\max}$	time when the droplet diameter reaches the maximum value
$\underline{u}$	local velocity vector
$u_{\rm in}$	velocity at inlet
u_γ	velocity vector for droplets, given by Eq. (8)

Greek symbols

β	artificial compressibility factor
γ	integer indicating the specific moment
$\dot{\gamma}$	local velocity gradient
γ_1, γ_2	specific values of γ
$\Delta S_\gamma^{br}(d)$	change in moments of distribution due to breakup
$\Delta S_\gamma^{cl}\,(d, d')$	change in moments of distribution due to collision
ε	porosity
η_c	viscosity of the continuous phase
λ	dummy value used in interpolation functions
μ	fluid viscosity
σ	interfacial tension
φ	volume fraction

sient (dynamic) behavior of the microstructure of such a mixture due to the high geometrical complexity of such a configuration. For example, the domain size could grow because the domains may coalesce under flow conditions and a break-up process sets in when they are large enough to be affected.

Renewed interest in this field originates from theoretical investigations on flow in porous materials using conventional computational aspects (Goldschmidt et al., 2003; Mousavi et al., 2006; Štěpánek and Ansari, 2005), the lattice Boltzmann method (Inamuro, 2006; Luo and Girimaji, 2002, 2003), and pore network sim-

ulators (Bravo et al., 2006; Fenwick and Blunt, 1998). These approaches focus mainly on the dynamics of flow for multiphase and multicomponent fluids rather than the microstructure formation where very limited effort has been focused (Kostoglou and Karabelas, 1994, 2005; Lehr et al., 2002; Luo and Svensen, 1996; Wang et al., 2003).

This theoretical study aims at the description of this microstructuring, especially for a mixture flowing in a homogeneous porous medium under laminar conditions. In particular, the scope of this theoretical study is to investigate the physical/geometrical parameters as well as the flow conditions which could assure the homogeneity of the mixture (water/droplets, i.e., continuous/discontinuous phase) in terms of mean droplet size. The focus is on the domain sizes formed during this process, and the approach we take is the so-called "$S\gamma$ concept", i.e., the "moments of distribution", for the description of the droplet sizes as in Kamp et al. (2001), where an arbitrary number of moments of the domain size distribution is used to describe the microstructure. In the same study, the method was also described in relation to experiments on bubble coalescence. Subsequently, Klahn et al. (2002) and Agterof et al. (2003) used that method for the analysis of experiments on the transient behavior of emulsion droplet breakup in an impeller flow and analysis of the behavior of double emulsions, respectively. All examples showed the power of the method, which will be explained in some detail below.

Summarizing, we extend the $S\gamma$ method to phenomena related with porous structures. The problem we examine is the laminar flow of a biphasic mixture in a homogeneous porous medium. The domain size for the two phases not only depends on the flow itself but also on the break-up and coalescence processes taking place because of the flow. The fundamental idea of the method is that the evolution of the moments of a distribution can be analyzed using a transport equation including a convective term, which can be coupled to the local flow characteristics, which should not be affected by the presence of droplets. It is evident that this assumption is valid only for droplet sizes small enough to follow the bulk flow and to adequately assure the homogeneity of the flowing mixture [see Eq. (8) and the relative detailed discussion there]. The source terms in the transport equation describe the local phenomena (breakup and coalescence) that affect the particle size distribution. The main advantage of this approach is that analytical expressions (including probabilistic parameters) for the characteristic magnitudes could be derived, leading to successful simulations through common and rather simple computational fluid dynamics (CFD) techniques.

2. THEORY: THE MOMENTS OF DISTRIBUTION ($S\gamma$)

The domain (droplets) size distribution can be described by a collection of moments of the distribution as (Kamp et al., 2001; Klahn et al., 2002; Agterof et al., 2003)

$$S_\gamma = n \int_0^\infty d^\gamma \, P\,(d) \; \mathrm{d}d \tag{1}$$

where γ is an integer indicating the specific moment, n is the total number density, and $P(d)$ is the size distribution of the droplets. Some of these moments can be directly related to physical properties of the dispersion. More precisely (Kamp et al., 2001; Agterof et al., 2003),

$$S_0 = n \int_0^\infty P\,(d) \; \mathrm{d}d = n \tag{2a}$$

is the total number of droplets (number density),

$$S_2 = n \int_0^\infty d^2 \, P\,(d) \; \mathrm{d}d \tag{2b}$$

is the specific interfacial area, and

$$S_3 = n \int_0^\infty d^3 \, P\,(d) \; \mathrm{d}d = \frac{6\varphi}{\pi} \tag{2c}$$

is an expression for the volume fraction, φ.

It is easy to show that for two different γ values, the corresponding $S\gamma$ functions can produce a useful characteristic diameter $d_{\gamma_1\gamma_2}$ according to the relation

$$\begin{aligned} d_{\gamma_1\gamma_2} &= \left(\frac{\int_0^\infty d^{\gamma_1} \, P\,(d) \; \mathrm{d}d}{\int_0^\infty d^{\gamma_2} \, P\,(d) \; \mathrm{d}d} \right)^{\frac{1}{\gamma_1 - \gamma_2}} \\ &= \left(\frac{S_{\gamma_1}}{S_{\gamma_2}} \right)^{\frac{1}{\gamma_1 - \gamma_2}} \quad \text{for} \quad \gamma_1 \neq \gamma_2 \end{aligned} \tag{3}$$

The most interesting $d_{\gamma_1\gamma_2}$ is the area-weighted mean droplet diameter, d_{32}, given as

$$d_{32} = \frac{S_3}{S_2} = \frac{\int_0^\infty d \left[d^2 \, P\,(d) \right] \; \mathrm{d}d}{\int_0^\infty d^2 \, P\,(d) \; \mathrm{d}d} \tag{4}$$

This diameter is a spatially averaged size, which in the present study is considered to be representative for the actual droplet size.

The main advantage of the $S\gamma$ function is that it satisfies the transport equation (Kamp et al., 2001). Starting from the well-known population balance equation and by following the mathematical route presented in Kamp et al. (2001), one can derive the following transport equation:

$$\frac{\partial nP(d)}{\partial t} + \nabla \cdot (\underline{u} nP(d)) = G - E \tag{5}$$

where $\underline{u}$ is the local velocity vector and G and E are the generation and the extinction terms, respectively. These terms are strongly related to the creation (breakup) and death (coalescence) of droplets.

After multiplying each term by d^γ and subsequently integrating overall particle sizes, the following equation can be obtained:

$$\frac{\partial}{\partial t}\left[\int_0^\infty d^\gamma nP(d)\mathrm{d}d\right] + \nabla \cdot \left[n\int_0^\infty d^\gamma \underline{u} P(d)\mathrm{d}d\right] = \int_0^\infty (G-E)d^\gamma \mathrm{d}d \tag{6}$$

By reversing the order of differentiation and integration, this equation can also be written as a transport equation as follows:

$$\frac{\partial S_\gamma}{\partial t} + \nabla \cdot (u_\gamma S_\gamma) = h_i^{(\gamma)} \tag{7}$$

where

$$u_\gamma = \frac{\int_0^\infty P(d)u(d)d^\gamma \mathrm{d}d}{\int_0^\infty P(d)d^\gamma \mathrm{d}d} \tag{8}$$

The expression in (8) equals the local velocity vector, $\underline{u}$, if the droplets have the same velocity as the flowing continuous bulk phase, an assumption that is adopted in the present study. Actually, it has been assumed that the local flow field is independent of the droplets; thus, their mean diameter is very low to affect the homogeneity of the flowing phase. Even for porosities close to unity, the mean droplets size must be lower than 10^{-6} m for creeping or laminar flow conditions (Lehr et al., 2002) in order to satisfy the above assumption.

In Eq. (7), $h_i^{(\gamma)}$ is the source term related to droplet breakup and coalescence, expressed in terms of the moments of distribution. For the majority of engineering applications, the above transport equation could be simplified to

$$\frac{\partial S_\gamma}{\partial t} + \underline{u} \cdot \nabla S_\gamma = h_i^{(\gamma)} \tag{9}$$

As far as the flow problem could be uncoupled from the transport one, the velocity field $\underline{u}$ can be obtained from typical CFD flow simulations.

3. THEORY: DETERMINATION OF THE SOURCE TERMS

Since the governing phenomena in the fluid phase are the droplet breakup and coalescence processes, the source term of the previous equation can be expressed as

$$h_i^{(\gamma)} = h_{br}^{(\gamma)} + h_{cl}^{(\gamma)} \tag{10}$$

where $h_{br}^{(\gamma)}$ and $h_{cl}^{(\gamma)}$ are the respective source terms that can be modeled explicitly.

3.1 Breakup Source Term

Breakup happens when the droplet diameter becomes larger than a critical value, d_{cr}, related with the critical capillary number as follows:

$$d_{cr} = \frac{2\,\sigma\, Ca_{cr}}{\eta_c\,\dot{\gamma}} \tag{11}$$

where Ca_{cr} is the critical capillary number, $\dot{\gamma}$ is the local velocity gradient, η_c is the viscosity of the continuous phase, and σ is the interfacial tension. This critical diameter depends also on the viscosity ratio and the flow type, as discussed extensively elsewhere (Grace, 1982; Stone, 1994).

The break-up source term, in its generic form, can be written as (Janssen et al., 1994)

$$h_{br}^{(\gamma)} = \int_0^\infty K_{br}(d)\Delta S_\gamma^{br}(d) nP(d)\mathrm{d}d \tag{12}$$

where K_{br} is the break-up rate and $\Delta S_\gamma^{br}(d)$ is the change in $S\gamma$ due to a single break-up event of a droplet of size d. An expression for $\Delta S_\gamma^{br}(d)$ follows from the conservation of dispersed phase volume when droplet fragments are formed (Wieringa et al., 1996),

$$\Delta S_\gamma^{br}(d) = d^\gamma \cdot \left(N_f(d)^{\frac{3-\gamma}{3}} - 1\right) \tag{13}$$

where N_f is the number of fragments formed. Since the break-up rate K_{br} is conversely analogous to the break-up time τ_{br}, the break-up source term becomes

$$h_{br}^{(\gamma)} = \int_0^\infty \left[\frac{d^\gamma}{\tau_{br}(d)} \left(N_f(d)^{\frac{3-\gamma}{3}} - 1 \right) \right] nP(d)\,\mathrm{d}d \quad \text{for} \quad d > d_{cr} \tag{14}$$

3.2 The Coalescence Source Term

Coalescence depends not only on the collisions but also on the coalescence probability; thus, the generic form of the coalescence source term is (Chesters, 1991)

$$h_{cl}^{(\gamma)} = \int_0^\infty \int_0^\infty K_{cl}(d,d')\ \Delta S_\gamma^{cl}(d,d')\ n^2 \times P(d)\,P(d')\ \mathrm{d}d\,\mathrm{d}d' \tag{15}$$

where K_{cl} is the collision rate, whose detailed description follows. The change in $S\gamma$ due to a single coalescence event, $\Delta S_\gamma^{cl}(d,d')$, between two droplets of diameters d and d', respectively, can be expressed as (Chesters, 1991)

$$\Delta S_\gamma^{cl}(d,d') = d^\gamma \left[\left(1 + \left(\frac{d'}{d} \right)^3 \right)^{\gamma/3} - \left(1 + \left(\frac{d'}{d} \right)^\gamma \right) \right] \tag{16}$$

or, by involving a uniform distribution with an equivalent mean diameter d_{eq},

$$\Delta S_\gamma^{cl} = d_{eq}^\gamma \left(2^{\gamma/3} - 2 \right) \tag{17}$$

Consequently, the coalescence source term becomes (Agterof et al., 2003)

$$h_{cl}^{(\gamma)} = \left(2^{\gamma/3} - 2 \right) \left(\frac{6\varphi}{\pi} \right)^2 K_{cl}(d_{eq})\, d_{eq}^{\gamma-6} \tag{18}$$

The coalescence rate $K_{cl}(d_{eq})$ is typically given as (Chesters, 1991)

$$K_{cl}(d_{eq}) = K_{coll}(d_{eq})\ P_{coal}(d_{eq}) \tag{19}$$

where $P_{coal}(d_{eq})$ is the coalescence probability of a single collision event, which is a function of the equivalent diameter, d_{eq}, and $K_{coll}(d_{eq})$ is analogous to the product $k_{coll}u_{rel}(d_{eq})$, representing the Smoluchowski collision rate (Agterof et al., 2003). Finally, the coalescence source term is given as

$$h_{cl}^{(\gamma)} = \left(2^{\gamma/3} - 2 \right) \left(\frac{6\varphi}{\pi} \right)^2 k_{coll} u_{rel}(d_{eq}) \times P_{coal}(d_{eq})\, d_{eq}^{\gamma-4} \tag{20}$$

4. SIMULATIONS

The simulations were carried out using a FORTRAN code especially developed for this work. Calculations were performed on a simple PC equipped with an Intel© Duo Core processor and 2 GB of RAM using a Windows XP© operating system. On average, the calculations took about half a day.

4.1 The Algorithm

To adequately simulate the above-described problem, we used the algorithmic procedure shown in Fig. 1. The procedure we used is as follows: first we calculate the characteristics of the flow in a porous medium using standard CFD methods, and subsequently the local velocity field obtained is used in a transport equation for the analysis of the evolution of the domain size distribution. Although the algorithm aims at a steady-state solution, the moderate results up to its end could be used for the study of transient behavior of the mean droplets by just taking into account the steady-state flow field in any case. For the numerical solution of the transport boundary value problems, a nonuniform finite difference scheme with upwinding was used for discretization in space, with the resulting linear systems of equations solved again using successive over-relaxation (SOR).

4.2 The Domain

To define a realistic domain for the solution of the flow and transport problem, a porous medium is constructed in the form of a spherical particle assemblage. Specifically, the representation of the biphasic domains under consideration is achieved by the random deposition of spheres of a given radius in a box of specified dimensions as presented in Fig. 2, where a sample medium of $\varepsilon = 0.72$ is depicted. The structure is digitized and the phase function is determined to obtain the specified porosity. The size of the digitized domains is $102 \times 102 \times 102$, and the length of the simulation box is approximately 10 times the sphere radius.

4.3 The Flow Field

To obtain the velocity field, it is necessary to solve the Stokes equations,

$$\nabla p = \mu \nabla^2 \underline{u} \tag{21a}$$

$$\nabla \cdot \underline{u} = 0 \tag{21b}$$

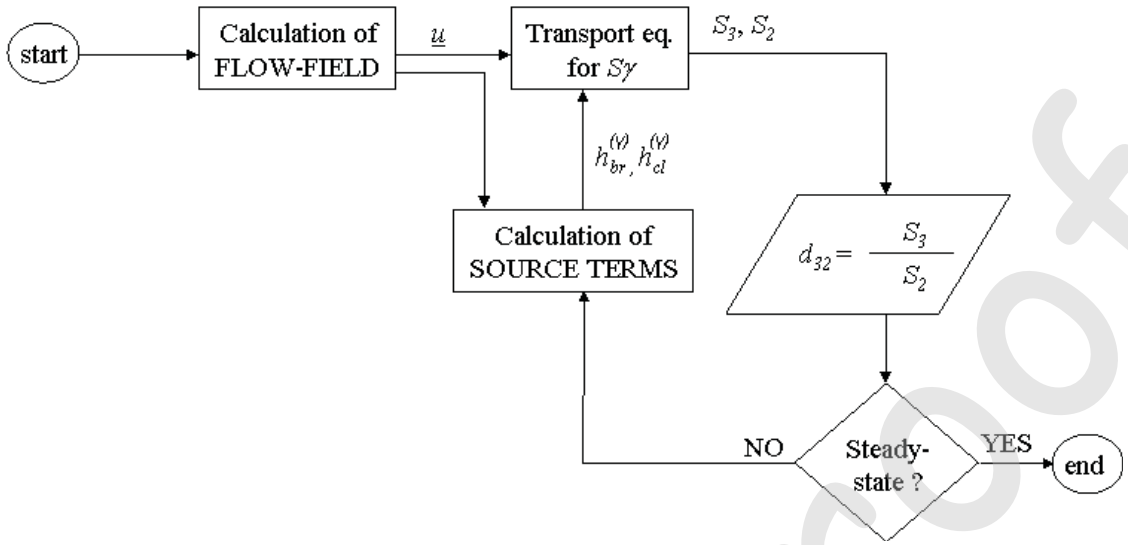

FIG. 1: Flowchart of the simulation algorithm

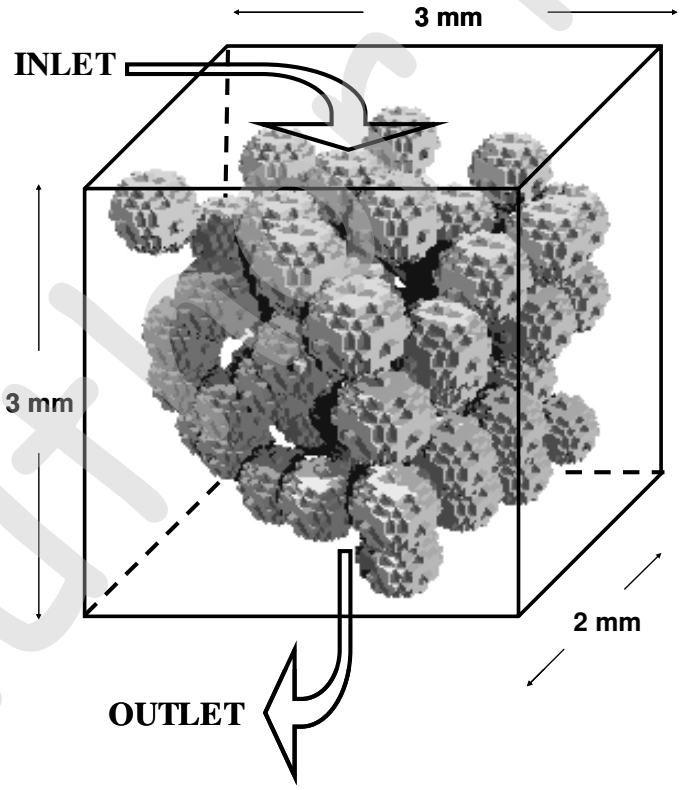

FIG. 2: Stochastically constructed 3-D porous medium

where $\underline{u}$, p, and μ are the velocity vector, the pressure field, and the fluid viscosity, respectively. The procedure for solving the three-dimensional Stokes flow problem is rather complicated in the vicinity of a porous structure (Kainourgiakis et al., 2002; Kikkinides and Burganos, 2000), where a staggered marker-and-cell (MAC) mesh is involved, with the pressure defined at the center of the cell and the velocity components defined along the corresponding face boundaries. The resulting linear system of equations is solved by an SOR method. An initial guess for p is determined through the solution of a Laplace equation. Next, the velocity vector $\underline{u}$ is calculated from the corresponding momentum balance and the continuity equation $\nabla \cdot \underline{u} = 0$. The pressure is corrected through an artificial compressibility equation of the form

$$\frac{dp}{dt} = \beta \nabla \cdot \underline{u} \tag{22}$$

Essentially, the method adds an artificial density time derivative related to the pressure by an artificial equation of state $p = \beta\rho$, where β is an artificial compressibility factor. In analogy with the compressible momentum equation, $c = \beta^{1/2}$ is an artificial speed of sound and thus, for stability reasons during the iterative procedure, its magnitude should be such that the respective artificial Mach number, $M = (R/c) \max_D \left(\sum_i u_i^2 \right)^{1/2}$, is low ($M \ll 1$), where R is the relevant Reynolds number. In the limiting case of $R \to 0$, which is the present case, any finite value of β should meet this criterion. Thus $\beta = 1$ was chosen, β although it is evident that the exact value cannot have any effect on the final (steady-state) results, since at steady state the artificial density time derivative is equal to zero. The above steps are repeated until convergence is reached. This numerical scheme for the determination of the velocity field has been widely validated in terms of both the velocity field and the corresponding permeability (Adler et al., 1990; Coutelieris et al., 2003).

5. INITIAL AND BOUNDARY CONDITIONS

One of the six surfaces of the simulated domain was considered to be an inlet, while the opposite one is assigned as outlet. The other four surfaces of the domain were assumed to be spatially periodic, both from a geometrical and physical (flow and transport) point of view.

The differential equations for the flow-field were integrated with the following initial and boundary conditions:

$$u(r, t = 0) = 0 \tag{23}$$

$$P(r, t = 0) = P_0 \tag{24}$$

$$u(r = \text{void space of the inlet}, t) = u_{\text{in}} \tag{25a}$$

$$\nabla \cdot u(r = \text{void space of the inlet}, t) = 0 \tag{25b}$$

$$P(r = \text{void space of the inlet}, t) = P_{\text{in}} \tag{26}$$

$$P(r = \text{void space of the outlet}, t) = P_0 \tag{27}$$

$$u(r = \text{void/solid interfaces}, t) = 0 \tag{28}$$

Initial conditions (23) and (24) indicate a quiescent mixture in void space of the porous medium, while boundary conditions (25a), (25b), and (26) impose a uniform (plug) flow at the inlet. Obviously, nonzero values appear only at the surfaces of the void space, since velocity and pressure are zero at the solid phase. Boundary condition (27) assures the necessary pressure gradient for the Stokes flow, while Eq. (28) expresses the no-slip condition at the fluid/solid interfaces, everywhere in the porous medium. Finally, spatial periodicity is assumed for pressure and velocity at the rest for outer surfaces of the domain.

The transport equation (9) was integrated with the following initial and boundary conditions:

$$S_\gamma(r, t = 0) = 10^{-16} \tag{29}$$

$$S_\gamma(r = \text{void space of the inlet}, t) = (S_\gamma)_{\text{in}} \tag{30a}$$

$$\nabla \cdot S_\gamma(r = \text{void space of the inlet}, t) = 0 \tag{30b}$$

$$S_\gamma(r = \text{void space of the outlet}, t) = (S_\gamma)_{\text{out}} \tag{31}$$

$$\nabla \cdot S_\gamma(r = \text{void/solid interfaces}, t) = 0 \tag{32}$$

Initial condition (29) indicates a very low initial population for droplets, while boundary conditions (30) and (31) impose a gradient for $S\gamma$. Equation (32) expresses neutral behavior at the fluid/solid interfaces, while spatial periodicity is again assumed for the other outer surfaces of the domain. Note that the above conditions are independent of the γ values.

5.1 Validation of the Algorithm

To examine the validity of the solution scheme, we have tested the algorithm against its consistency. More precisely, different sets of $S\gamma$ values should lead to broadly the same distribution parameters, i.e., to the same mean droplet size, by using Eq. (3). Such a test has been provided by carrying out simulations for two specific sets of $S\gamma$ values, namely, S_1, S_2, S_3, and S_4 These distributions lead to mean droplet sizes through $d_{32} = (S_3/S_2)$ and $d_{41} = (S_4/S_1)^{1/3}$, which should theoretically be the same. The mesh and time step size were the same for

both cases. Figure 3 depicts this comparison, where the two curves represent the evolution with time of d_{32} and d_{41}, respectively. Since the results are quite identical, this plot indicates the self-consistency of $S\gamma$ modeling.

6. RESULTS AND DISCUSSION

Since the droplet size is represented by d_{32}, the solution scheme is hereafter used only for $\gamma = 2$ and $\gamma = 3$; thus, the relevant source terms for the rest of this work become

$$h_{br}^{(2)} = \int_0^\infty \left[\frac{d^2}{\tau_{br}(d)} \left(\sqrt[3]{N_f(d)} - 1 \right) \right] nP\,(d)\,\mathrm{d}d \quad (33a)$$

$$h_{cl}^{(2)} = -0.740079 \left(\frac{6\varphi}{\pi} \right)^2 k_{coll} u_{rel}\,(d_{eq}) \times P_{coal}\,(d_{eq})\,d_{eq} \quad (33b)$$

$$h_{br}^{(3)} = 0 \quad (33c)$$

$$h_{cl}^{(3)} = 0 \quad (33d)$$

For the results presented here, the simulation's parameters are tabulated in Table 1. Note that since the aim of this study is the theoretical investigation of the transport process, the interpolation functions $f_1\,(\lambda)$ and $f_2\,(\lambda)$, used for the estimation of $N_f(d)$ and τ_{br}, were set to unity. For specific cases, these functions should be changed according to the experimental results available for these cases.

The time evolution of the averaged characteristic droplet size, d_{32}, is presented in Fig. 4 up to a critical time when the system reaches the steady-state situation. A maximum in this size is observed at $t = 550$ s, mainly due to the competition between the hydrodynamic phenomena, i.e., breakup and coalescence. Later at $t = 900$ s, the droplet size distribution levels off, taking a rather constant

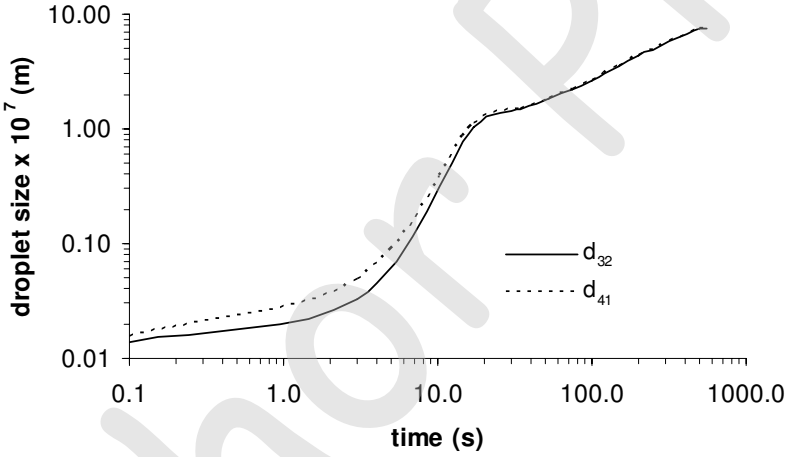

FIG. 3: Evolution of the averaged droplet size for two different sets of $S\gamma$ values

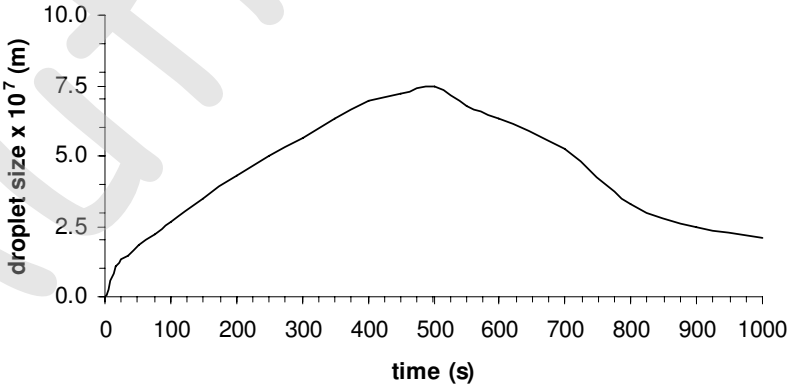

FIG. 4: Characteristic averaged droplet size (d_{32})

TABLE 1: Parameters used in the simulations

Parameter	Units	Expression/value	Reference/comment
$N_f(d)$	(-)	$2.69 f_1(\lambda)\left(\frac{d}{d_{cr}}\right)^3$	(Grace, 1982)
$\tau_{br}(d)$	(s)	$\frac{2\eta_c d}{\sigma} f_2(\lambda)$	(Grace, 1982)
$f_1(\lambda), f_2(\lambda)$	(-)	• 1 for the current case • other values/expressions for the specific case studied	
d_{cr}	(m)	Eq. (11)	Calculated at each point and time step
σ	(N m^{-1})	0.0728	Since the current work is purely theoretical, the continuous phase is supposed to be water
Ca_{cr}	(-)	1	(Mingzhe et al., 1998)
η_c	(Centipoises)	0.89	Since the current work is purely theoretical, the continuous phase is supposed to be water
$P(d)$	(-)	$\frac{1}{d\hat{\sigma}\sqrt{2\pi}}\exp\left(-\frac{\left(\ln d - \ln \overline{d}\right)^2}{2\,\hat{\sigma}^2}\right)$	(Kamp et al., 2001)
$\hat{\sigma}$	(-)	0.1	(Chesters, 1991; Kamp et al., 2001)
$\overline{d}$	(m)	3×10^{-8}	(Chesters, 1991; Kamp et al., 2001)
$k_{coll} u_{rel}(d_{eq})$	(m s^{-1})	$0.6667\underline{u}$	(Chesters, 1991; Kamp et al., 2001)
$P_{coal}(d_{eq})$	(-)	Follows the log-normal distribution according to the droplet diameters	(Chesters, 1991; Kamp et al., 2001)
d_{eq}	(m)	$\left(\frac{6\varphi}{\pi S_\gamma}\right)^{\frac{1}{3-\gamma}}$	(Agterof et al., 2003)
φ	(-)	$\frac{4}{3}\pi\left(d_{32}\right)^3 \frac{1}{0.03 \times 0.03 \times 0.02} n$	Calculated at each time step
n	(m^{-3})	Whole algorithm and Eq. (2a)	Calculated once from the solution for S_0

value for longer time scales. This dynamic behavior of the system is clarified in Fig. 5, where the relative significance of the source terms is shown. The individual source terms have been normalized by their maximum value, i.e., $h_{br}^{(\gamma)} = h_{br}^{(\gamma)}/\mathrm{MAX}\left\{h_{br}^{(\gamma)}\right\}$, $h_{cl}^{(\gamma)} = h_{cl}^{(\gamma)}/\mathrm{MAX}\left\{h_{cl}^{(\gamma)}\right\}$, in order to fit the same graph. Actually, their initial values are nonzero because the model assumes that the evolution of the droplet size initiates from a nonzero value as well (see Fig. 4). During the first 550 s, coalescence dominates over the breakup as the particles are quite small; therefore, the droplet sizes increase. At $t = 550$ s the contributions of breakup and coalescence are balanced and thus, the particle size goes through a maximum. After 550 s, breakup becomes more significant than coalescence and thus, the particle size decreases up to $t = 900$ s. The time considered for the simulation is critical for the validity of the results. Obviously, this critical simulation time is strongly dependent on the specific medium's geometry and the flow characteristics. Therefore the simulation time for the above presented results is $t = 1000$ s for the given porosity ($\varepsilon = 0.72$) and velocity field ($u = 1$ m/s). A more detailed study of the influence of these parameters follows below, where steady-state results are going to be presented.

Although porosity is not directly involved in the specified transport equations, it is a crucial parameter for the microstructure transport phenomena since it significantly affects the local flow field and the mass-transport regime through the void space in the porous medium. Thus, its effect is clearly presented in Figs. 6 and 7. The time instant when the droplet diameter reaches the maximum value, $t_{\max}$, is presented in Fig. 6 as a function of the medium's porosity. The variation of $t_{\max}$ with porosity seems to be low because the droplets size is much

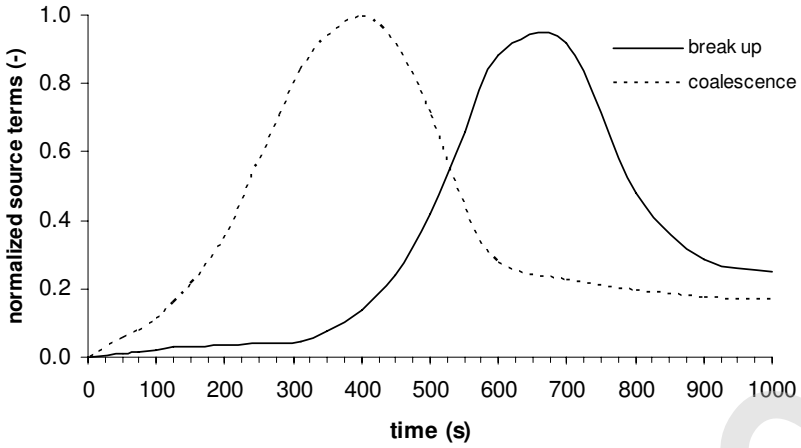

FIG. 5: Relative significance of source terms

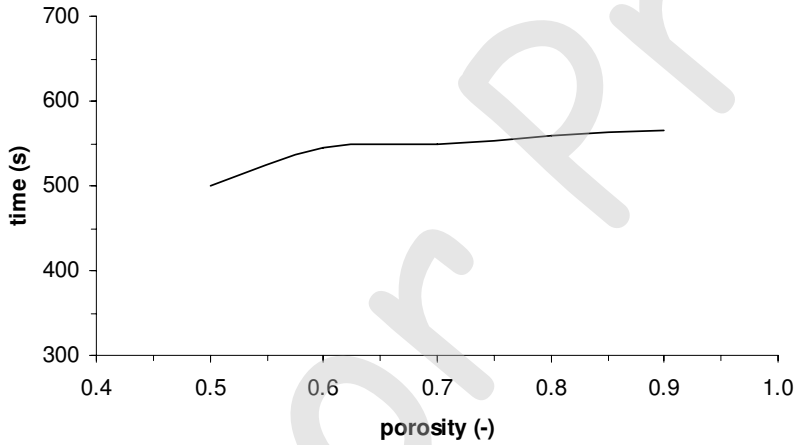

FIG. 6: Effect of porosity on the time when MAX$\{d_{32}\}$ is observed

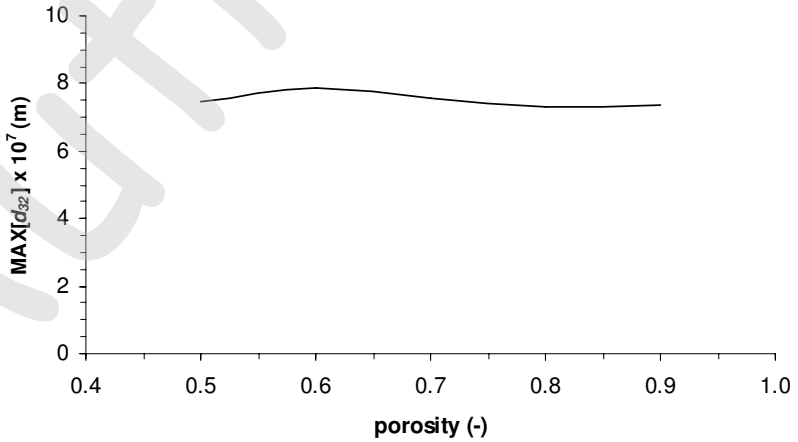

FIG. 7: MAX$\{d_{32}\}$ as a function of porosity

smaller than the mean pore diameter, therefore leaving the droplets affected by the presence of the solid phase, even for the lowest porosity value. Furthermore, lower values of porosity correspond to higher coalescence probabilities because the lower the porosity, the narrower the path for a bubble to escape without any collision and therefore, the higher the coalescence source term. In addition, breakup is not significantly affected by porosity, because $h_{br}^{(\gamma)}$ is nonzero only for diameters higher than a critical diameter value, whose order of magnitude is 10^{-7} m, which corresponds to porosity values of order of magnitude 10^{-5} for reasonable characteristic length. Obviously, the actual porosity values are in the range of 0.5–0.9, assuring that $h_{br}^{(\gamma)}$ is not practically affected by the porosity. Therefore, the only influence of the decreasing porosity is the enhancement of $h_{br}^{(\gamma)}$, which corresponds to earlier times for maximum diameters with lower porosity. However, this influence on $t_{\max}$ does not correspond to any significant change of the absolute value of maximum diameter, as depicted in Fig. 7. Indeed, the maximum values of source terms remain rather unaffected by the porosity, leading to a maximum diameter that varies little, despite the fact that the time when these maximum values occur varies with porosity, as discussed previously.

Figures 8 and 9 show the effect of flow intensity on the droplet size. As it can be observed in Fig. 8, an increase in the inlet velocity value corresponds to delayed times when the maximum diameter appears. Indeed, as veloc-

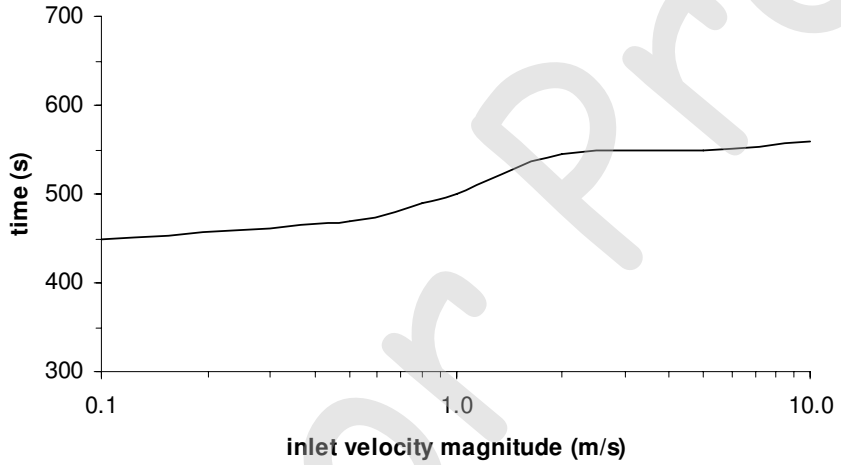

FIG. 8: Effect of inlet velocity magnitude on the time when MAX$\{d_{32}\}$ is observed

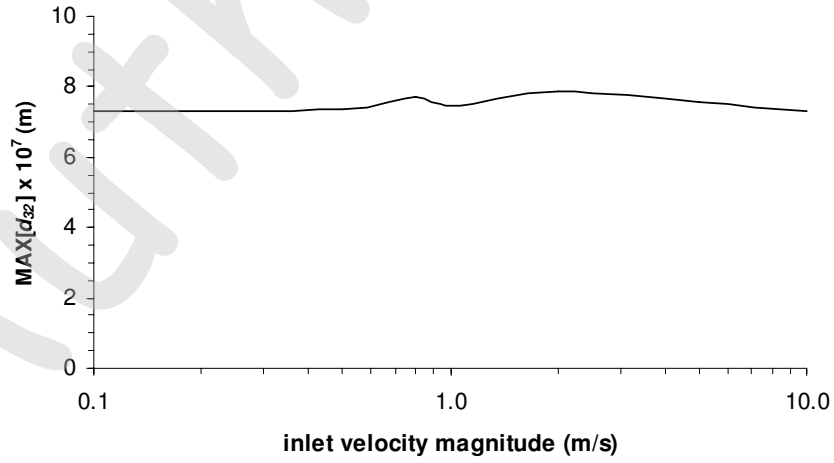

FIG. 9: MAX$\{d_{32}\}$ as a function of inlet velocity magnitude

ity increases, i.e., convection dominates over diffusion, it is easier for the droplets to collide and, therefore, the coalescence source term increases. Furthermore, a very low increment for the break-up source term also is expected because the higher the velocity, the easier for a droplet to reach and interfere with the solid phase. Since the phenomenon dominantly influenced by the flow is coalescence, maximum diameter is observed later for higher convective regimes. Again, this does not seem to significantly affect the magnitude of this maximum diameter (Fig. 9) for the same reasons as those discussed above.

7. CONCLUSIONS

In the present work, the "$S\gamma$ concept" has been applied to predict the microstructure formation (in terms of the time evolution of the averaged droplet size) in a mixture flowing in a homogeneous porous medium. This microstructure formation process is governed by the competition between local hydrodynamic phenomena, i.e., breakup and coalescence of bubbles. At the early part of the process, coalescence dominates over breakup, leading to a significant incremental increase of the average droplet size. Since breakup becomes competitive at later stages, it is observed that it starts decreasing up to a value dependent on geometrical and flow parameters, i.e., porosity and inlet velocity. Of special importance is the occurrence of a maximum in the droplet diameter which is observed when breakup and coalescence show an equivalent contribution to the process. Furthermore, it is found that the time when this maximum occurs is strongly dependent on these parameters (porosity, inlet velocity) while its magnitude is not.

ACKNOWLEDGMENTS

The author would like to thank Dr. A. Stubos for his useful assistance in the discussion of the results.

REFERENCES

Adler, P. M., Jacquin, C. J., and Quiblier, J. A., Flow in simulated porous media, *Int. J. Multiphase Flow*, vol. **16**, pp. 691–712, 1990.

Agterof, W. G. M., Vaessen, G. E. J., Haagh, G. A. A. V., Klahn, J. K., and Janssen, J. J. M., Prediction of emulsion particle sizes using a computational fluid dynamics approach, *Colloid Surface B*, vol. **31**, pp. 141–148, 2003.

Bravo, M. C., Araujoc, M., and Lago, M., Pore network modeling of two-phase flow in a liquid-(disconnected) gas system, *Physica A*, vol. **375**, pp. 1–17, 2007.

Chesters, A. K., The modeling of coalescence processes in fluid–liquid dispersions, *Chem. Eng. Res. Des.*, vol. **69**, pp. 259–270, 1991.

Coutelieris, F. A., Kainourgiakis, M. E., and Stubos, A. K., Low Peclet mass transport in assemblages of spherical particles for two different adsorption mechanisms, *J. Colloid Interface Sci.*, vol. **264**, pp. 20–29, 2003.

Fenwick, D. H. and Blunt, M., Three-dimensional modeling of three phase imbibition and drainage, *Adv. Water Resour.*, vol. **21**, pp. 121–143, 1998.

Gerami, S. and Pooladi-Darvish, M., Predicting gas generation by depressurization of gas hydrates where the sharp-interface assumption is not valid, *J. Petrol. Sci. Eng.*, vol. **56**, pp. 146–164, 2007.

Goldschmidt, M. J. V., Weijers, G. G. C., Boerefijn, R., and Kuipers, J. A. M., Discrete element modelling of fluidized bed spray granulation, *Powder Technol.*, vol. **138**, pp. 39–45, 2003.

Grace, H. P., Dispersion phenomena in high-viscosity immiscible fluid systems and application of static mixers as dispersion devices in such systems, *Chem. Eng. Commun.*, vol. **14**, pp. 225–277, 1982.

Heibel, A. K., Scheenen, T. W. J., Heiszwolf, van As, J. J., Kapteijn, H. F., and Moulijn, J. A., Gas and liquid phase distribution and their effect on reactor performance in the monolith film flow reactor, *Chem. Eng. Sci.*, vol. **56**, pp. 5935–5944, 2001.

Inamuro, T., Lattice Boltzman methods for viscous fluid flows and for two-phase fluid flows, *Fluid Dyn. Res.*, vol. **38**, pp. 641–659, 2006.

Janssen, J. J. M., Boon, A., and Agterof, W. G. M., Influence of dynamic interfacial properties on droplet break-up in simple shear flow, *AIChE J.*, vol. **40**, pp. 1929–1939, 1994.

Kainourgiakis, M. E., Kikkinides, E. S., and Stubos, A. K., Diffusion and flow in porous domains constructed using process-based and stochastic techniques, *J. Porous Mater.*, vol. **9**, pp. 141–154, 2002.

Kamp, A. M., Chesters, A. K., Colin, C., and Fabre, J., Bubble coalescence in turbulent flows: A mechanistic model for turbulence-induced coalescence applied to microgravity bubbly pipe flow, *Int. J. Multiphase Flow*, vol. **27**, pp. 1363–1396, 2001.

Kikkinides, E. S. and Burganos, V. N., Permeation properties of three-dimensional self-affine reconstructions of porous materials, *Phys. Rev. E*, vol. **62**, pp. 6906–6915, 2000.

Klahn, J. K., Janssen, J. J. M., Vaessen, G. E. J., de Swart, R., and Agterof, W. G. M., On the escape process during phase inversion of an emulsion, *Colloid Surface A*, vol. **210**, pp. 167–181, 2002.

Kostoglou, M. and Karabelas, A. J., Evaluation of zero order methods for simulating particle coagulation, *J. Colloid Interface Sci.*, vol. **163**, pp. 420–431, 1994.

Kostoglou, M. and Karabelas, A. J., Induced pulsing in trickle beds, Characteristics and attenuation of pulses, *Chem. Eng. Sci.*, vol. **60**, pp. 6584–6595, 2005.

Lehr, F., Millies, M., and Mewes, D., Bubble-size distributions and flow fields in bubble columns, *AIChE J.*, vol. **48**, pp. 2426–2443, 2002.

Luo, L. S. and Girimaji, S. S., Lattice Boltzmann model for binary mixtures, *Phys. Rev. E*, vol. **66**, pp. 035301/1-035301/4, 2002.

Luo, L. S. and Girimaji, S. S., Theory of the lattice Boltzmann method: Two-fluid model for binary mixtures, *Phys. Rev. E*, vol. **67**, pp. 036302/1-036302/11, 2003.

Luo, L. S. and Svensen, H. F., Theoretical model for drop and bubble breakup in turbulent dispersions, *AIChE J*., vol. **42**, pp. 1225–1233, 1996.

Mingzhe, D., Dullien, F., and Jun, Z., Characterization of water-flood saturation profile histories by the "complete" capillary number, *Transp. Porous Media*, vol. **31**, pp. 213–237, 1998.

Mousavi, S. M., Jafari, A., Yaghmaei, S., Vossoughi, M., and Sarkomaa, P., Computer simulation of fluid motion in a porous bed using a volume of fluid method: Application in heap leaching, *Miner. Eng*., vol. **19**, pp. 1077–1083, 2006.

Sheng, J. J., Hayes, R. E., Maini, B. B., and Torkite, W. S., Modelling foamy oil flow in porous media, *Transp. Porous Media*, vol. **35**, pp. 227–258, 1999.

Štěpánek, F. and Ansari, M. A., Computer simulation of granule microstructure formation, *Chem. Eng. Sci*., vol. **60**, pp. 4019–4029, 2005.

Stone, H. A., Dynamics of drop deformation and break up in viscous fluids, *Annu. Rev. Fluid Mech*., vol. **26**, pp. 65–102, 1994.

Wang, T., Wang, J., and Jin, J., A novel theoretical breakup kernel function of bubble/droplet in a turbulent flow, *Chem. Eng. Sci*., vol. **59**, pp. 2593–2595, 2003.

Wieringa, J. A., van Dieren, F., Janssen, J. J. M., and Agterof, W. G. M., Droplet break-up mechanism during emulsification in colloid mills at high dispersed fraction, *Inst. Chem. Engl.*, vol. **74**, pp. 554–562, 1996.